Eur. Phys. J. D **33**, 243–251 (2005)
DOI: 10.1140/epjd/e2005-00037-5

THE EUROPEAN PHYSICAL JOURNAL D

Vibrational excitation and negative ion production in radio frequency parallel plate H_2 plasmas

P. Diomede, S. Longo[a], and M. Capitelli

Dipartimento di Chimica dell'Universita' di Bari, Via Orabona 4, 70126 Bari, Italy
and
IMIP/CNR, Sez. Bari, Via Orabona 4, 70126 Bari, Italy

Received 16 December 2004
Published online 12 April 2005 –

Abstract. A theoretical study of the vibrational kinetics and attachment in low pressure hydrogen plasmas produced by Radio Frequency (RF) discharges is performed. In particular we study the influence of gas/surface kinetic processes such as the vibrational deactivation and the atomic recombination of molecules. The production of vibrationally excited molecules by the surface recombination of atoms is also considered. The study is realized by means of a self-consistent one dimensional kinetic model, and a parallel plate RF discharge test case is implemented. Results show that surface processes are able to affect the vibrational distribution function (vdf) and the negative ion (H^-) density. The effect of vibrational exothermicity of H atom recombination is also discussed as a way to reduce the gap between theory and experimental results. Moreover, it is shown that the H^- ion heating by the electric field strongly affects the detachment rate: this effect is specially important for negative ions produced through Rydberg states in this kind of discharges.

PACS. 52.20.-j Elementary processes in plasmas – 52.65.-y Plasma simulation – 52.50.Dg Plasma sources

1 Introduction

The chemical kinetics of non equilibrium, low pressure hydrogen discharge plasmas is important in view of both the theoretical value of this test case, for the special position of hydrogen in physics and chemistry, and the several important applications of gas discharges in pure hydrogen and mixtures of hydrogen with other gases.

A study of these systems has been performed by different theoretical methods; most of the models for hydrogen developed until now are 'fluid' models [1–3] based on a macroscopic description of the charged particle kinetics in the discharge. Other are particle models, but do not take into account a detailed vibrational kinetics and its influence on H^- ions [4].

The most important features of the chemical/physical model to be reminded, in order to introduce the present study are:

(1) negative ions in the plasma are produced via electron impact dissociative attachment from vibrationally excited molecules (VDA) reactions

$$e^- + H_2\,(v = 0, \ldots, 14) \rightarrow H + H^- \qquad (1)$$

which are characterized by high cross-sections for vibrationally excited hydrogen molecules. Basically the peak cross-sections increase by five orders of magnitude when the molecule is vibrationally excited;

(2) a strong superthermal plateau in the vdf (vibrational distribution function) of hydrogen molecules is produced in the mid-dissociation range due to the EV processes

$$\begin{aligned} e^- + H_2\left(X^1\Sigma_g^+, v_i\right) &\rightarrow e^- + H_2\left(B^1\Sigma_u^+, C^1\Pi_g\right) \\ &\rightarrow e^- + H_2\left(X^1\Sigma_g^+, v_f\right) + h\nu \end{aligned} \qquad (2)$$

(i.e. electronic excitation followed by radiative decay to the X state, with a characteristic vibrational energy yield associated to the Franck-Condon factors);

(3) the same region of the vdf is depressed by VT energy exchange in collision of molecules with H atoms

$$H_2\,(v) + H \rightarrow H_2\,(w) + H \qquad (3)$$

(4) H atoms are mostly produced by electron-molecule collisions and by the ion conversion reaction

$$H_2^+ + H_2 \rightarrow H_3^+ + H \qquad (4)$$

and mostly lost by heterogeneous recombination on the electrode surfaces.

[a] e-mail: s.longo@chimica.uniba.it

The possibility of producing vibrationally excited molecules as a result of atom recombination was never considered in the previous works, also by other authors, in spite of the very high exothermicity, because of the lack of data. Recent studies [5] suggest that actually a relevant yield of vibrationally excited states will arise in the recombination of H atoms on metal surfaces. Since the quantitative aspects are still to be investigated, and also they are expected to be strong functions of the surface composition, temperature and crystallographic/metallurgical features, we propose here a parametric study based on the self-consistent model described below.

We will also compare our results with recent experimental measurements of negative ion yield on a real RF device: a preliminary comparison seems to add indirect evidence to the hypothesis that H atoms actually recombine on vibrationally excited levels.

A study of surface effects in H_2 plasmas has been performed in the past by Amorim et al. [6,7]. While this study was very comprehensive in its own terms, it was limited by assuming a uniform plasma, which can be described by coupling a quasi isotropic Boltzmann equation with a 0D plasma kinetics. A rigorous description of the surface effects should indeed consider the plasma disuniformity that is necessarily induced by the electrical and chemical properties of the surfaces. For this reason we use here a fully kinetic one dimensional model for the plasma. Furthermore, we consider in this study the possibility of atom recombination on vibrationally excited molecules.

Finally a simplified treatment of Rydberg states kinetics is implemented and it is found that in RF discharges, because of the presence of the ambipolar potential well, the detachment process is extremely dependent on the production region of H^- ions, so Rydberg states may be not effective in the H^- net yield.

2 Method of calculation

2.1 Charged particles kinetics

A 1D(r)2D(v) fully self-consistent particle/continuum model has been developed to study capacitively coupled RF discharge plasmas in hydrogen. The code includes a state-to-state reaction diffusion model [8], i.e. we solve at the same time the electron transport and chemical kinetic problems taking into account their reciprocal connection.

During the calculations, the densities of different species will be updated by solving appropriate equations. The approach is different for charged and neutral particles.

To solve the problem we use a Particle in Cell/Monte Carlo (PIC/MC) method for the transport equation and a grid-discretized relaxation technique for the reaction-diffusion part. In the PIC/MC, applied to electrons and four ionic species (H_3^+, H_2^+, H^+ and H^-), the Newton equation for a large ensemble of mathematical point particles is solved taking into account the local electric field as it results from local interpolation within a cell of a mathematical mesh.

Electron/neutral collisions have been included by the null collision Monte Carlo method, while ion/neutral processes have been implemented through a new null collision Monte Carlo method that considers the thermal distribution of neutrals [9].

Recombination processes cannot fit the basic PIC/MC formalism since they involve two charged particles. These processes are treated as a combination of two first order ones, each including one of the two particle species involved in the process.

The differential statistical weighting technique for H^+ ions already described in [8] is here extended to other ions (H^- and H_2^+) in order to improve the statistics of the results. Moreover, an additional ad hoc technique has been implemented in order to speed up the convergence of the negative ion kinetics: we scale both α (the H^- production rate) and β (the loss frequency per H^- particle) to $k\alpha$ and $k\beta$ respectively, with $k > 1$, while keeping $n(H^-) = \alpha/\beta$ constant. This implies scaling the cross-sections for attachment and detachment, and the rate coefficients in the treatment of H^- recombination. The technique works since electrons and other ion densities are not affected significantly by attachment or H^- detachment. This has been checked by direct comparison with code results with $k = 1$ [10].

2.2 Neutral species kinetics

The density for the neutral species n_c is obtained by finding a stationary solution for the set of non-linear rate equations with a diffusion term that in one dimension reads as:

$$-D_c \frac{\partial^2 n_c(x)}{\partial x^2} = \sum\nolimits_r (\nu'_{rc} - \nu_{rc})\, k_r\, (\langle f_e \rangle_t) \prod\nolimits_{c'} n_{c'}^{\nu_{rc}} \quad (5)$$

where D_c is the diffusion coefficient and ν_{rc} is the molecularity of the cth species in the rth elementary process.

After any calculation step of the motion equations, the electric charge in any cell of the mesh is determined from the number of electrons and ions found in the cell itself, according to their statistical weight. Known the electric charge density, the electric potential and field are determined by solving the Poisson equation on the mesh.

The electron-molecule process rate coefficients k_r in equation (5) are calculated as a function of the position taking into account f_e, the electron energy distribution function (eedf):

$$k_r(x) = \sqrt{\frac{2}{m_e}} \int_0^\infty \varepsilon f_e(\varepsilon, x) \sigma(\varepsilon) d\varepsilon \quad (6)$$

where σ is the process related total cross-section and m_e and ε are the electron mass and energy.

The set of reaction-diffusion equations is numerically solved at the steady state on a mathematical grid by a Gauss/Seidel technique.

2.3 Gas/surface kinetics

The processes occurring on the walls are considered in the boundary conditions. In our model, the reactions considered are the vibrational deactivation of molecules, with probability $\gamma_{\rm V}$, and the pseudo-first-order H recombination on the wall surface, with probability γ_H

$$\mathrm{H_2\,(X}, v>0) - (\mathrm{wall}) \rightarrow \mathrm{H_2\,(X}, v=0)$$

$$\mathrm{H} - (\mathrm{wall}) \rightarrow \frac{1}{2}\mathrm{H_2\,(X}, v=0)\,. \quad (7)$$

The catalytic boundary conditions can be written as:

$$D_{\mathrm{H_2}}\frac{\partial n_{\mathrm{H_2}(v=1,\ldots,14)}}{\partial\zeta} = \frac{\gamma_{\rm V}}{4}\left(\frac{8kT_g}{\pi m_{\mathrm{H_2}}}\right)^{1/2} n_{\mathrm{H_2}(v=0,\ldots,14)} \quad (8)$$

$$D_{\mathrm{H}}\frac{\partial n_{\mathrm{H}}}{\partial\zeta} = \frac{\gamma_{\mathrm{H}}}{4}\left(\frac{8kT_g}{\pi m_{\mathrm{H}}}\right)^{1/2} n_{\mathrm{H}} \quad (9)$$

where ζ is the coordinate normal to the surface, k is the Boltzmann constant, T_g is the gas temperature, D is the diffusion coefficient and $n_{\mathrm{H_2}(v=0,\ldots,14)}$ and n_{H} are the densities close to the surface.

The deactivation of higher vibrational levels that are important for negative ions production is mainly controlled by VT collisions with H atoms. The concentration of H atoms strongly depends on the wall recombination probability γ_{H}, which is linked to the corresponding wall recombination frequency, in the case of a first-order wall mechanism, by the expression

$$\nu_{\mathrm{H}} = \frac{\gamma_{\mathrm{H}} v_{\mathrm{th}}(\mathrm{H})}{4d} = \frac{\gamma_{\mathrm{H}}}{4d}\sqrt{\frac{8kT_g}{\pi m_{\mathrm{H}}}} \quad (10)$$

where v_{th} is the H thermal velocity, d is the discharge gap and m_{H} is the hydrogen atom mass. Unfortunately, the choice of the γ_{H} value is always uncertain, because it depends on the nature of surface, on the wall temperature and on discharge parameters. This explains the large discrepancies found in literature for the experimental value of γ_{H}. In our case, we assume that the recombination probability of H atoms on the walls is an input parameter. Similar problems arise concerning the molecules vibrational deactivation probability $\gamma_{\rm V}$.

In most previous works it was assumed that the recombination of atomic hydrogen produces molecules in their ground vibrational state. However, due to the high energy involved in the recombination reaction, it was reported in the literature [5] that the recombination actually delivers vibrationally excited molecules. Further test cases were carried out in order to check the effect of different assumptions concerning this point. To simplify we have assumed that one single excited vibrational level is produced, according to the reaction

$$\mathrm{H} - (\mathrm{wall}) \rightarrow \frac{1}{2}\mathrm{H_2\,(X}, v')\,. \quad (11)$$

This feature is included by extending the boundary condition formalism, by adding the following term to the right side of equation (8)

$$-\delta_{vv'}\gamma_{\mathrm{H}} v_{\mathrm{th}}(\mathrm{H}) n_{\mathrm{H}}/8 \quad (12)$$

that differs from equation (9) for a factor 2 that accounts for stoichiometry.

2.4 Negative ion production through Rydberg states

We checked the effect of including in the attachment kinetics Rydberg states, whose importance has been underlined in multicusp and microwave sources [11,12].

A simplified implementation of the Rydberg states kinetics has been carried out by multiplying the sum cross-section for electron impact excitation to Rydberg states [13] by a weighting factor:

$$W_{Ryd} = \frac{n_e K_{RDA}}{n_e K_{RDA} + \tau^{-1}} \quad (13)$$

where n_e is the space-averaged electron number density, K_{RDA} is the dissociative attachment from Rydberg states (RDA) rate coefficient, that we consider equal to 5×10^{-5} cm^3 s^{-1}, after Pinnaduwage et al. [14], and τ^{-1} is the radiative decay frequency, equal to 10^6 s^{-1}, after Garscadden et al. [12]. The weighting factor is obtained from the steady-state approximation applied to the reaction scheme:

$$e + \mathrm{H_2} \rightarrow e + \mathrm{H_2^R} \quad (14)$$

$$\mathrm{H_2^R} \rightarrow \mathrm{H_2} + h\nu \quad (15)$$

$$\mathrm{H_2^R} + e \rightarrow \mathrm{H} + \mathrm{H^-}. \quad (16)$$

The weighted cross-section is used for the treatment of the RDA process, that produces H^-, but at the same time, the weight takes into account the radiative decay of the Rydberg states.

3 Case study, results and discussion

3.1 Test case

Like in the references cited above, we consider as a case study the parallel plate radio frequency discharge (RF) which is well described by an axial one-dimensional model when the diameter of the plates is larger than the discharge gap (i.e. the distance between the two plates). In this case our computational domain is the fraction of the discharge axis between $x = 0$ and $x = d$, d being the discharge gap. The boundary conditions for the electric potential are $V(0) = 0$ and $V(d) = V_{rf}\sin(2\pi\nu_{rf}t)$, where V_{rf} is the discharge voltage and ν_{rf} is the RF frequency.

We consider as a test case the following physical conditions: gas temperature 300 K, voltage amplitude 300 V, gas pressure 1 torr, discharge frequency 13.56 MHz, discharge gap 0.02 m, DC voltage (bias) 0 V, as in reference [15].

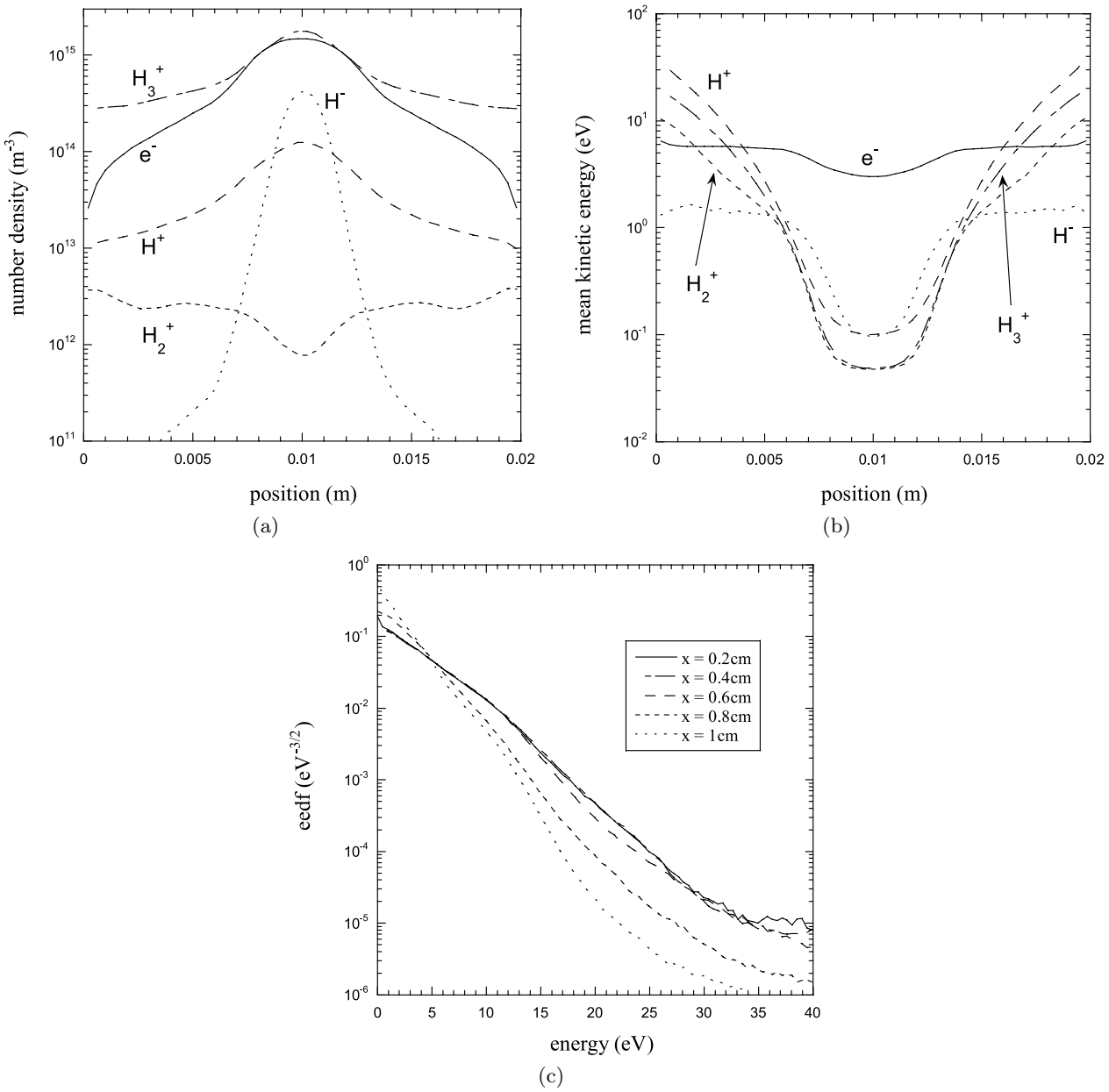

Fig. 1. (a) Charged particle number density as a function of position calculated using average values for the probability parameters ($\gamma_{\rm V} = 0.02$, $\gamma_{\rm H} = 0.2$); $V_{rf} = 300$ V, $p = 1$ torr, $\nu_{rf} = 13.56$ MHz, $d = 0.02$ m. (b) Charged particle mean kinetic energy as a function of position for the test case. (c) Electron energy distribution function as a function of energy in different positions in the discharge.

3.2 Effect of accommodation probabilities

In Figure 1 plasma quantities, with values for the probability parameters ($\gamma_{\rm V} = 0.02$, $\gamma_{\rm H} = 0.2$) calculated as a geometric average of the data found in literature [16–20], are shown, in particular: (a) number density, (b) mean kinetic energy of charged species as a function of position and (c) electron energy distribution function (eedf) as a function of energy. All the quantities have been time averaged during a sampling time $\Delta t_{sampling}$, which is the time interval between two calls of the chemical kinetics module and is typically 2×10^5 time steps, while the time step value is 5×10^{-11} s. In order to save CPU time, a particle is selected for the sampling with 10% probability at every time step.

From Figure 1a the known phenomenology of discharge plasmas is retrieved: the plasma is neutral in the center (bulk) region while two positive regions (the sheaths) develop in contact to the electrode surface, following the absorption of a fraction of the electrons, which move considerably faster than ions in the plasma. Also it must be noted how negative ions accumulate in the very center of the discharge by dropping into the self-generated ambipolar potential well. The presence of negative ions in the center of the discharge produces a partially electronegative

Table 1. $n_{H-}(m^{-3})$ in the discharge center for different values of the probability parameters γ_V and γ_H (V_{rf} = 300 V, p = 1 torr, ν_{rf} = 13.56 MHz, d = 0.02 m).

γ_V \ γ_H	0.01	0.2	1
0	4.70×10^{13}	1.05×10^{15}	1.39×10^{15}
0.02	3.22×10^{13}	3.17×10^{14}	3.91×10^{14}
0.5	2.98×10^{13}	2.78×10^{14}	3.33×10^{14}
1	2.92×10^{13}	2.75×10^{14}	3.38×10^{14}

Table 2. Tv_{0-1}(K) in the discharge center for different values of the probability parameters γ_V and γ_H (V_{rf} = 300 V, p = 1 torr, ν_{rf} = 13.56 MHz, d = 0.02 m).

γ_V \ γ_H	0.01	0.2	1
0	1560	1811	1830
0.02	996	1011	1012
0.5	767	769	769
1	755	757	757

region in the center of the plasma, which affects the distributions of minoritary ions (especially H_2^+). Figure 1b shows the space distribution of the time averaged energy for charged particles: as expected positive ions are thermalized to the gas temperature in the bulk while they reach fairly high energies in the proximity of the electrode surfaces, while negative ions, which are confined in the center of the discharge, do not reach such high energies. Electrons, which are not effectively thermalized by collisions with the gas medium, have an energy of a few eV in the bulk plasma, and reach a higher energy in the sheath region. Anyway, the collisional kinetics of electrons cannot be determined, as known, from the mean energy only, but an account of the full eedf is in order. This last is reported in Figure 1c, which shows that the eedf significantly deviates from the Maxwell-Boltzmann law and the most relevant feature is the long 'tail' at energy >15 eV. This structure is due to the interaction of a small electron fraction with the high electric field in the sheath region, since only electrons above the ambipolar potential barrier can be accelerated by the sheath field. The presence of this superthermal tail in the eedf favors the production of highly vibrationally excited molecules through the high threshold EV processes.

We performed a parametric study of the influence of the hydrogen atom wall recombination probability and hydrogen molecule wall deactivation probability on the H^- concentration and on the quantities related to it, such as the vibrational temperatures Tv_{0-1} (estimating the molecules vibrational energy amount) and Tv_{0-7} (that indicates the position of the vdf plateau and is calculated based on the number densities of levels $v = 0$ and $v = 7$). All these quantities are calculated in the center of the discharge and are shown in Tables 1–3.

From Table 1 it can be noticed that the highest yield of negative ions results when the walls are non catalytic as regards vibrational deactivation ($\gamma_V = 0$) and fully catalytic as regards atomic recombination ($\gamma_H = 1$). The vibrational temperatures obtained by the self-consistent method are relatively low with respect to the electron temperature (about 3 eV in the bulk discharge plasma) due to the strong wall deactivation effects, as shown by the strong influence of the vibrational deactivation, while the bulk atomic VT deactivation modulated by γ_H through the atomic density is less critical, specially at high values of γ_V (see Tab. 2). This result is consistent with the experiments in reference [21] in which the vibrational temperature is lower than 2000 K. Of course the temperature associated to the levels 0 to 7 population ratio (Tab. 3) is higher, witnessing the plateau featured by the vibrational distribution (see discussion below).

Table 3. Tv_{0-7}(K) in the discharge center for different values of the probability parameters γ_V and γ_H (V_{rf} = 300 V, p = 1 torr, ν_{rf} = 13.56 MHz, d = 0.02 m).

γ_V \ γ_H	0.01	0.2	1
0	2521	2760	2795
0.02	2490	2570	2575
0.5	2412	2477	2480
1	2400	2465	2470

In Figures 2a–2d is reported a comparison between the dissociative attachment events occurring during the interval $\Delta t_{sampling}$ defined above and the corresponding vibrational distribution function (vdf) as a function of the vibrational level quantum number of the hydrogen molecule in two different situations among the many considered in the parametric study of the wall catalytic properties. In the first (Figs. 2a and 2b), we considered non catalytic walls for the vibrational deactivation ($\gamma_V = 0$) and we varied γ_H: this variation strongly influences the position of the vdf plateau and consequently the dissociative attachment events histogram, while the Tv_{0-1} remains almost unchanged. In the second case (Figs. 2c and 2d), we considered a low value for the wall recombination probability ($\gamma_H = 0.01$) and we varied γ_V, realizing an influence on the Tv_{0-1} temperature and a strong drop of the dissociative attachment events for the levels with $v > 1$, with respect to the previous case, together with a weak influence on this last diagram. It should be noted that the vdf is calculated in the center of the discharge.

3.3 Effect of the recombination level

Table 4 reports the results obtained for H^- ions, H atom and electron concentration in the discharge center, varying the vibrational level of recombination of the H atoms on the walls.

It can be noticed that the level of recombination has a strong influence on H^- concentration, while the other quantities are not considerably affected. In this case we consider $\gamma_V = 0.02$ and $\gamma_H = 0.2$, which are geometric averages of experimental values found in literature as explained before.

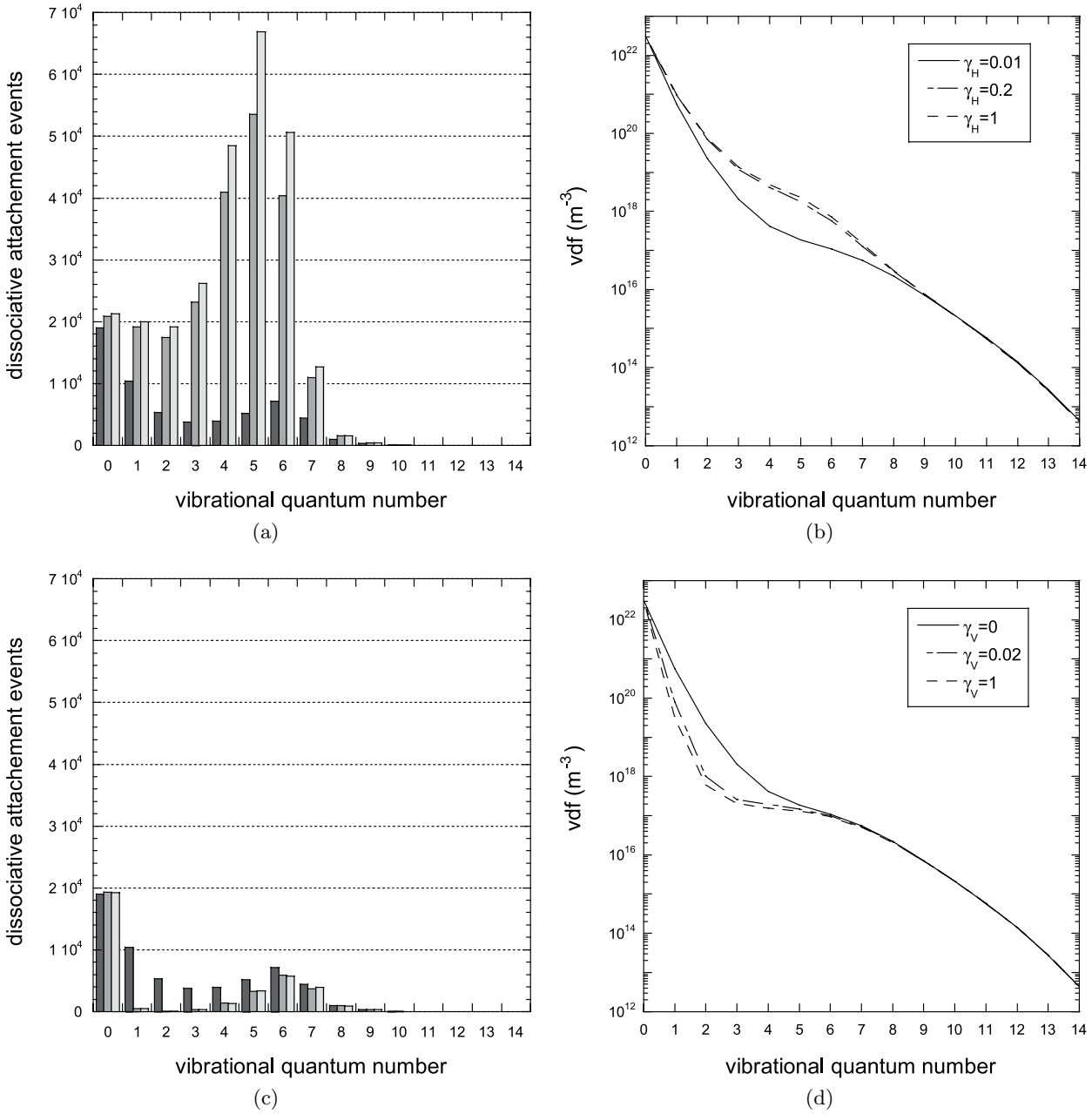

Fig. 2. (a) Dissociative attachment events as a function of the vibrational quantum number for $\gamma_{\rm V} = 0$ and different values of $\gamma_{\rm H}$: 0.01 (dark grey column), 0.2 (grey column), 1 (light grey column). (b) Vibrational distribution function in the discharge center as a function of the vibrational quantum number for the same conditions of (a). (c) Dissociative attachment events as a function of the vibrational quantum number for $\gamma_{\rm H} = 0.01$ and different values of $\gamma_{\rm V}$: 0 (dark grey column), 0.02 (grey column), 1 (light grey column). (d) Vibrational distribution function in the discharge center as a function of the vibrational quantum number for the same conditions of (c).

Table 4. Influence of the H_2 vibrational level of recombination of H atoms (V_{rf} = 300 V, p = 1 torr, ν_{rf} = 13.56 MHz, d = 0.02 m) on H^-, H and electron number density in the discharge center ($\gamma_{\rm V} = 0.02$, $\gamma_{\rm H} = 0.2$).

	$n_{\rm H^-}$ (m^{-3})	$n_{\rm H}$ (m^{-3})	n_e (m^{-3})
$v = 0$	3.17×10^{14}	7.3×10^{18}	1.15×10^{15}
$v = 7$	5.72×10^{14}	7.4×10^{18}	1.18×10^{15}
$v = 14$	6×10^{14}	7.4×10^{18}	1.18×10^{15}

Figure 3 illustrates the effect of the vibrational level of surface recombination on the vibrational distribution function in two different positions in the discharge, near the electrodes (Fig. 3a) and in the center of the discharge (Fig. 3b). It can be noticed a raising of the plateau with the recombination level and a modification of the shape of the curves near the electrodes, for the levels $v > 7$. The effect on the negative ion production can be observed in Figure 3c, that shows that the largest variation occurs

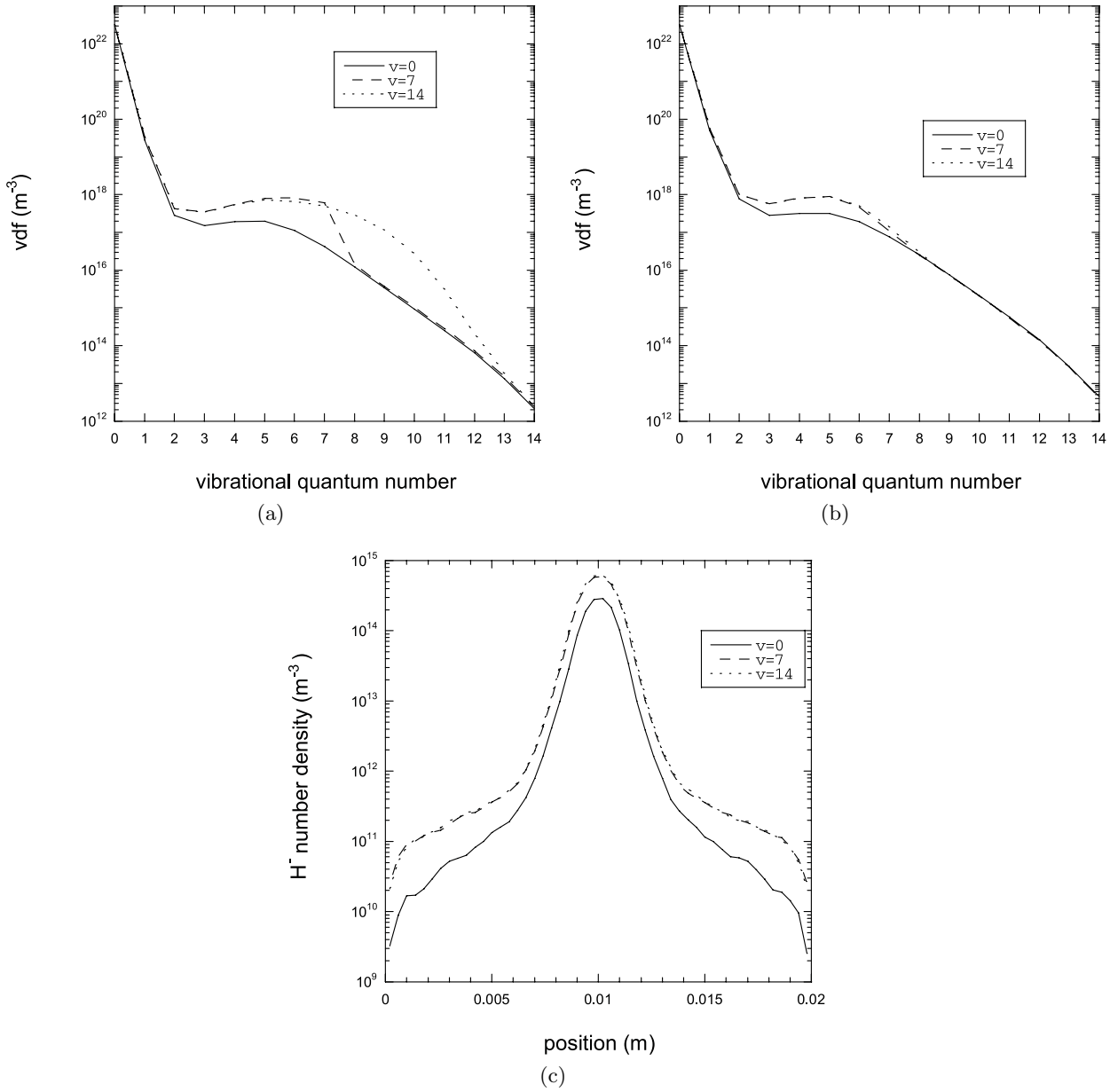

Fig. 3. (a) Vibrational distribution function as a function of the vibrational quantum number in the position $x = 0.2$ cm in the discharge, for surface atom recombination on the $v = 0$ level (solid line), $v = 7$ (dashed line), $v = 14$ (dotted line), ($\gamma_V = 0.02$, $\gamma_H = 0.2$). (b) Vibrational distribution function as a function of the vibrational quantum number in the position $x = 1$ cm in the discharge, for surface atom recombination on the $v = 0$ level (solid line), $v = 7$ (dashed line), $v = 14$ (dotted line), ($\gamma_V = 0.02$, $\gamma_H = 0.2$). (c) H^- number density as a function of the position in the discharge, for surface atom recombination on the $v = 0$ level (solid line), $v = 7$ (dashed line), $v = 14$ (dotted line), ($\gamma_V = 0.02$, $\gamma_H = 0.2$).

in the sheath region, while, in the plasma center, the influence of the recombination level is modest, since the largest variation of the vdf occurs in the sheath region, where the electron density is very low, while the tail of the vdf in the course of molecule diffusion to the bulk plasma is promptly depressed by VT processes.

Table 5 illustrates the same quantities of Table 4, but with value of the hydrogen atom wall recombination probability and hydrogen molecule wall deactivation probability forced in order to obtain the maximum value of H^- concentration and to fit its experimental value [15]: $\gamma_V = 0$, $\gamma_H = 1$. It can be noticed that a good agreement is obtained in this case. Of course this result has been obtained with somewhat extreme assumptions concerning the surface properties: this assumptions could be likely relaxed in future studies with a particle kinetics even more complex than the quite comprehensive one used so far, including new channels boosting the production of negative ions, e.g. through a kinetics of electronic states and radiation.

Table 5. Influence of the H atoms recombination level (V_{rf} = 300 V, p = 1 torr, ν_{rf} = 13.56 MHz, d = 0.02 m) on H^-, H and electron number density in the discharge center ($\gamma_V = 0$, $\gamma_H = 1$). The experimental result in reference [15] for the H^- density is 5×10^{15} m^{-3}.

	n_{H^-} (m^{-3})	n_H (m^{-3})	n_e (m^{-3})
$v = 0$	1.39×10^{15}	6.4×10^{18}	1.21×10^{15}
$v = 7$	2.98×10^{15}	7.2×10^{18}	1.54×10^{15}
$v = 14$	3.1×10^{15}	7.2×10^{18}	1.60×10^{15}

Note also that in these extreme conditions the negative ion concentration exceeds that of the electrons emphasizing the electronegative behavior of the discharge.

3.4 Effect of Rydberg state kinetics

Figure 4a shows the H^- number density and production rates, as a function of the position in the discharge, for the test case with average values of the wall catalysis probabilities ($\gamma_V = 0.02$, $\gamma_H = 0.2$) and atoms that recombine in the $v = 0$ level, with and without considering Rydberg states kinetics. It can be noticed that the H^- density is not affected sensibly by the insertion of Rydberg states processes. This result contrasts with those of previous homogeneous model calculations [11,12] asking for an explanation. Actually the RDA production rate strongly exceeds the VDA rate as shown in Figure 4a; at the same time, a strong increase of the detachment channel

$$H^- + H_2 \rightarrow H_2 + H + e^- \qquad (17)$$

compensates for the increase in the H^- production channel. The enhancement in the detachment rate can be explained as a joint effect of a raising in the H^- kinetic energy and the fact that the related cross-section [22] rises fast to very large values for energies above the threshold at 2.37 eV.

In Figure 4b, the H^- kinetic energy calculated as a function of the position with and without considering Rydberg states kinetics is displayed. As can be seen, the mean kinetic energy of H^- ions is actually increased in the first case in the side regions. This last effect can be easily explained: the RDA ion production channel, as shown in Figure 4a, is effective specially in the side regions because high energy electrons are required to produce the Rydberg states. As a consequence of being produced in the side regions of the discharge, the negatively charged H^- ions gain kinetic energy by falling downhill the ambipolar potential energy well. This conspiracy of collisional and electrostatic effects explains how the RDA channel may be not effective in enhancing the H^- concentration in this kind of discharges. Of course this picture could be strongly modified in the future by the inclusion of additional cooling channels for negative ions (e.g. through inelastic collisions).

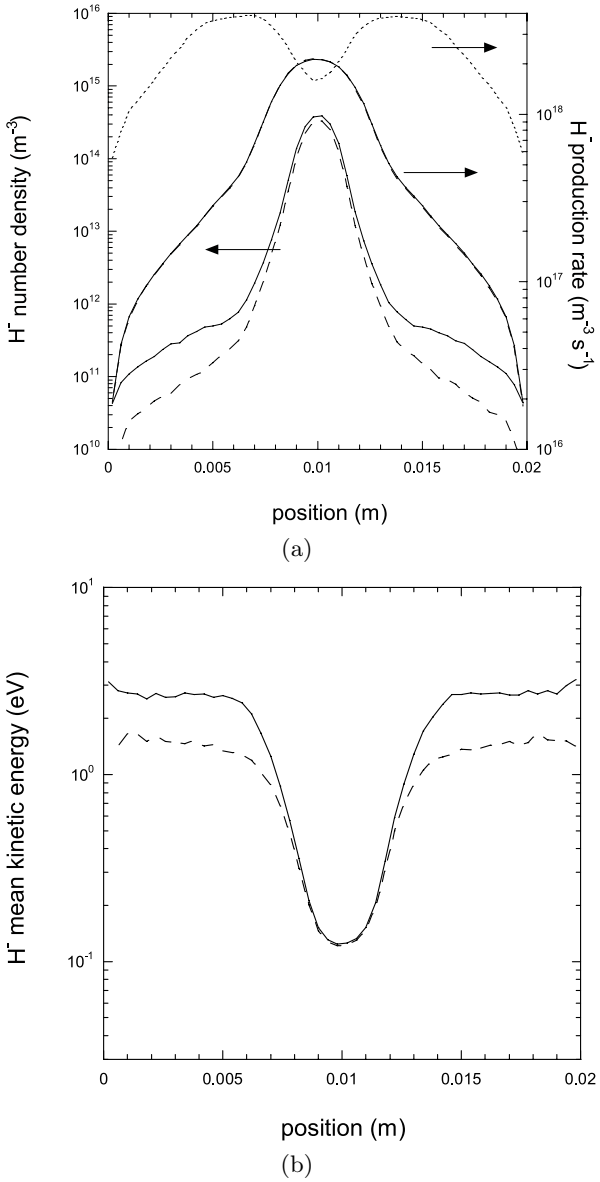

Fig. 4. (a) H^- number density and production rates as a function of the position in the discharge (V_{rf} = 300 V, p = 1 torr, ν_{rf} = 13.56 MHz, d = 0.02 m, γ_V = 0.02, γ_H = 0.2): with (solid line) and without (dashed line) considering Rydberg states kinetics. The RDA rate is represented by the dotted line. (b) H^- mean kinetic energy as a function of position in the discharge with (solid line) and without (dashed line) considering Rydberg states kinetics (V_{rf} = 300 V, p = 1 torr, ν_{rf} = 13.56 MHz, d = 0.02 m, γ_V = 0.02, γ_H = 0.2).

4 Conclusions

We have studied several aspects of the kinetic modelling of vibrational excitation and negative ion production in capacitively coupled parallel plate Radio Frequency discharges in hydrogen. The study has been performed by using a fully self-consistent 1D(r)2D(v) simulation code, which includes plasma dynamics and gas phase and

gas/surface chemical kinetics under a state-to-state approach. The values of the two reaction probabilities γ_V and γ_H affect the vdf and the plasma quantities in a complex way, due to the interaction of several kinetic issues which can only be described by a self-consistent approach.

Future studies should discuss in more detail the effect of excited H atoms and electronically excited molecules, as well as additional ionization channels, which have not yet been included and could help to reproduce the experimental results.

We found that the production of vibrationally excited molecules through the recombination of atoms on surfaces may have an important effect on the vdf and n_{H-}. We also studied in this context the debated issues of the possible role of attachment processes via Rydberg states, finding that the ions produced through this channel are mostly detached while falling into the ambipolar potential well. The detection of additional cooling channels could change this statement.

In conclusions, we believe that these issues should always be taken into account in the theoretical study of low pressure hydrogen plasmas, prior to claiming a good reproduction of experimental data, specially for what concerns the negative ion yield.

This work was partially supported by MIUR (project no. 2003037912_010) and ASI (pro. no. I/R/055/02). The calculations were performed in the framework of the GRID-FIRB project.

References

1. T. Novikova, B. Kalache, P. Bulkin, K. Hassouni, W. Morscheidt, P. Roca i Cabarrocas, J. Appl. Phys. **93**, 3198 (2003)
2. J.P. Boeuf, L.C. Pitchford, SIGLO-RF, PC version 1.0, a 1D User-Friendly Model for RF Discharges Simulation (Kinema Software, `siglo@kinema.com`, `http://www.siglo-kinema.com/siglo-rf.htm`, Monument, CO), 1995
3. A. Salabas, L. Marques, J. Jolly, G. Gousset, L.L. Alves, J. Appl. Phys. **95**, 4605 (2004)
4. K. Radouane, B. Despax, M. Yousfi, J.P. Couderc, E. Klusmann, H. Meyer, R. Shulz, J. Schulze, J. Appl. Phys. **90**, 4346 (2001)
5. E. Molinari, M. Tomellini, Chem. Phys. **270**, 439 (2001)
6. J. Loureiro, J. Amorim, Chem. Phys. **232**, 141 (1998)
7. J. Amorim, J. Loureiro, D. Schram, Chem. Phys. Lett. **346**, 443 (2001)
8. S. Longo, I.D. Boyd, Chem. Phys. **238**, 445 (1998)
9. S. Longo, P. Diomede, Eur. Phys. J. AP **26**, 177 (2004)
10. S. Longo, M. Capitelli, P. Diomede, Lect. Notes Comp. Sci. **3039**, 580 (2004)
11. K. Hassouni, A. Gicquel, M. Capitelli, Chem. Phys. Lett. **290**, 502 (1998)
12. A. Garscadden, R. Nagpal, Plasma Sources Sci. Technol. **4**, 268 (1995)
13. A.V. Phelps, Directory FTP `/collision_data/` in `jila.colorado.edu`
14. P.G. Datskos, L.A. Pinnaduwage, J.F. Kielkopf, Phys. Rev. A **55,** 4131 (1997)
15. B. Kalache, T. Novikova, A. Fontcuberta i Morral, P. Roca i Cabarrocas, W. Morscheidt, K. Hassouni, J. Phys. D: Appl. Phys. **37**, 1765 (2004)
16. A.M. Karo, J.R. Hiskes, R.J. Hardy, J. Vac. Sci. Technol. A **3**, 1222 (1985)
17. V.L. Orkin, V.G. Fedotov, A.M. Chaikin, Kinet. Catal. **18**, 55 (1977)
18. P. Kae-Nune, J. Perrin, J. Jolly, J. Guillon, Surf. Sci. **360**, L495 (1996)
19. C. Gorse, M. Capitelli, J. Bretagne, M. Bacal, Chem. Phys. **93**, 1 (1985)
20. B.J. Wood, H. Wise, J. Phys. Chem. **65**, 1976 (1961)
21. V.A. Shakhatov, O. De Pascale, M. Capitelli, Eur. Phys. J. D **29**, 235 (2004)
22. A.V. Phelps, J. Phys. Chem. Ref. Data **19** 653 (1990)